Japanese Journal of Applied Physics

Optimized Process of Mn^{2+}-Doped $Ba_{0.5}Sr_{0.5}TiO_3$ Thin Films on Platinum Coated Sapphire Substrates

To cite this article: Bin Zhu *et al* 2012 *Jpn. J. Appl. Phys.* **51** 035505

Japanese Journal of Applied Physics **51** (2012) 035505 **REGULAR PAPER**
DOI: 10.1143/JJAP.51.035505

Optimized Process of Mn^{2+}-Doped $Ba_{0.5}Sr_{0.5}TiO_3$ Thin Films on Platinum Coated Sapphire Substrates

Bin Zhu, Shuwen Jiang, Chengtao Yang, Ping Li, and Jihua Zhang*

State Key Laboratory of Electronic Thin Films and Integrated Devices, University of Electronic Science and Technology of China, Chengdu 610054, China

Received August 7, 2011; accepted December 18, 2011; published online February 27, 2012

Mn^{2+}-doped $Ba_{0.5}Sr_{0.5}TiO_3$ (BST) thin films were prepared on Pt-coated sapphire substrates by RF magnetron sputtering. By analyzing the energy state of particles during the sputtering, deposition parameters (substrate temperature, sputtering power, and atmosphere) were optimized for superior dielectric properties. Our results indicated that a compromise of relatively high tunability and low loss could be achieved. Resultant BST thin films has a tunability of 50% and dielectric loss of 0.64% at an applied field of 1.2 MV/cm, under optimized sputtering conditions of substrate temperature at 750 °C, pressure at 4 Pa with an $O_2/(O_2 + Ar)$ mixing ratio of 50%, and sputter RF power density at 6.8 W/cm^2.

1. Introduction

$Ba_xSr_{1-x}TiO_3$ (BST) thin films have been extensively investigated for applications in tunable devices due to their electric field dependent permittivity.[1–4] For tunable microwave devices, low dielectric loss as well as high tunability is essentially required. Though BST thin films perform relatively large dielectric tunability, the high dielectric loss (generally >1%) is a crucial limitation for practical utilizations.[5] In order to reduce the dielectric loss of BST thin films, great efforts have been made in the past decades, such as film texturing,[6–8] improvement of dielectric–electrode interface,[9,10] alteration/control of film stress,[11,12] modification of composition,[13–17] and photon irradiation[18] are applied. It has bee thought that Mn^{2+} ions doping may be an effective way to compensate oxygen vacancy defects in BST thin films thus to reduce the dielectric loss.[14,19] However, in case of widely applied parallel plate capacitors with metal–BST–metal (MIM) configuration, Mn^{2+} doped BST films usually perform high dielectric loss. For example, Kim *et al.*[20] and Subramanyam *et al.*[21] reported that the Mn^{2+}-doped BST thin films deposited on Pt and MgO substrates demonstrated a large dielectric loss of 1.58 and 3.3%, respectively. As the Mn substitution prevents the reduction of Ti^{4+} to Ti^{3+}, the dielectric loss of Mn^{2+}-doped $Ba_{0.7}Sr_{0.3}TiO_3$ thin films rise to 6.5% at 1 MHz.[22]

In fact, beside composition, the dielectric properties of the thin films also depend strongly on the deposition conditions. For example, it is thought that the dielectric loss of BST films in MIM configuration results mainly from the effect of interfacial diffusion between thin film and bottom electrode.[23] Up to now, a lot of efforts have been made to improve the dielectric properties of pure BST thin films by optimization sputtering conditions. However, the relation between sputtering conditions and dielectric properties of Mn-doped BST thin films has not been reported systematically yet. Therefore, although Mn-doped BST is promising, deposition process must be optimized before one can obtain high performances.

In this paper, the growth conditions of Mn-doped BST film are optimized for superior electrical properties. We firstly analyzed the energy states of particles during sputtering process, then experimentally evaluated the effect of variations of sputtering conditions such as substrate temperature, RF power and sputtering atmosphere on the electrical properties of BST thin film parallel capacitors. By balancing these sputtering factors with the goal of minimizing dielectric loss, we achieved the Mn^{2+}-doped BST thin films combining relatively high tunability with low loss on Pt-coated sapphire substrates.

Table I. Sputtering conditions for BST thin films.

Dimensions of chamber (mm)	ϕ450
Background pressure (Pa)	5×10^{-4}
Deposition pressure (Pa)	2–5
Gas ratio $O_2/(O_2 + Ar)$ (%)	15, 30, and 50%
RF power density (W/cm^2)	4.1–6.8
Target composition	2 mol % Mn-doped $Ba_{0.5}Sr_{0.5}TiO_3$
Target size (mm)	ϕ50
Target–substrate distance (mm)	80
Substrate temperature (°C)	550–800
Substrate material	Pt/Ti/sapphire (0001)

2. Experiments

BST thin films described in this work were RF magnetron sputtered after a bottom electrode (Ti/Pt, 20/100 nm) was dc sputtered on (0001)-oriented sapphire substrates at 200 °C. The sputtering targets were stoichiometric 2 mol % Mn^{2+}-doped $Ba_{0.5}Sr_{0.5}TiO_3$ ceramics. To optimize the sputtering parameters, the surface temperature of the sapphire substrates was varied from 550 to 800 °C. The RF power was changed ranging from 100 to 200 W, corresponding to power density of 3.4 to 6.8 W/cm^2. The sputtering ambient was a mixture of Ar and O_2 with the O_2/Ar flow rates in series of 7.5/42.5, 15/35, and 25/25 sccm, corresponding to $O_2/(O_2 + Ar)$ mixing ratio (OMR) of 15, 30, and 50%. The total sputtering pressure was controlled with a valve from 2 to 5 Pa. The RF magnetron sputtering conditions are summarized in Table I.

The growth time for all depositions was 2 h, resulting in film thicknesses ranging from 80 to 150 nm as measured by cross-section scanning electron microscopy (SEM). The crystal structure of the deposited BST films was examined using a Bede D1 X-ray diffraction (XRD) instrument. The film surface morphology was studied by a Seiko SPA-300HV atomic force microscope (AFM). For electrical

*E-mail address: jhzhang@uestc.edu.cn

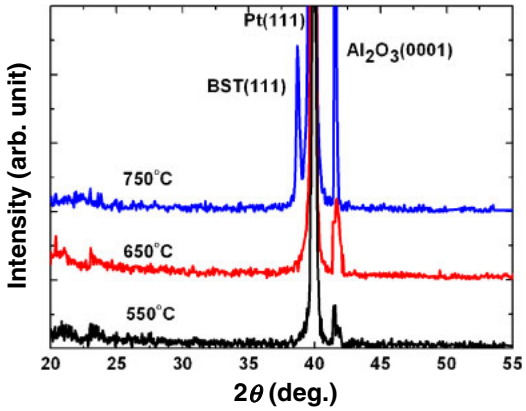

Fig. 1. (Color online) XRD patterns of Mn^{2+}-doped BST films sputtered at different substrate temperature.

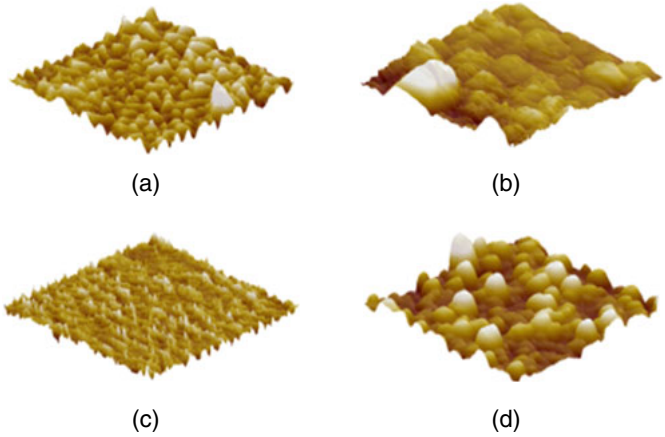

Fig. 2. (Color online) AFM surface morphologies of Pt electrodes annealed at (a) 550 °C, $R_a = 6.8$ nm, (b) 650 °C, $R_a = 6.5$ nm, (c) 750 °C, $R_a = 3.6$ nm, and (d) 800 °C, $R_a = 10.2$ nm.

measurements, Au top electrodes in diameter of 400 μm were evaporated on the surface of BST thin films through a shadow mask. The capacitance–voltage (C–V) properties of testing samples were investigated at 0.1 V AC voltage and 10 kHz by an Agilent HP4284A high precision LCR meter. All tests were carried out at room temperature.

3. Results and Discussion

Besides the chemical constituent, properties of film are highly related to film crystallization and interfacial structure. In general, BST thin films combining good integrity of crystallization with less interfacial diffusion performed better dielectric properties. On the basis of the sputtering energy process, the deposition conditions corresponding to RF power, sputtering atmosphere and substrate temperature can be evaluated to satisfy the energy states of particles. Basically, carefully selected sputter power, sputtering pressure and O_2/Ar ratio at appropriate substrate temperature would favor the good crystal integrity as well as less interfacial diffusion, thus improved dielectric properties.

3.1 Effect of substrate temperature

High substrate temperature is undoubtedly helpful for arranging of thin films since more energy can be provided to particles. However, interfacial diffusion between Pt electrodes and BST thin films will be enhanced significantly at a higher substrate temperature, which would increase the dielectric loss.[23,24] In the meanwhile, small hills may be formed on Pt electrode surface due to the mismatching of thermal expansion coefficient between platinum and sapphire substrates. Therefore, the role of substrate temperature on BST thin films needs a compromise. Figure 1 shows the crystal structure of BST films deposited at different substrate temperature. It can be seen that no BST peaks can be detected at 550 and 650 °C. With the substrate temperature increased to 750 °C, the films were found to be well crystallized with a (111)-preferred orientation. On the other hand, high substrate temperature would enhance the interfacial diffusion between BST thin films and Pt electrode, and the surface of Pt electrode may roughen due to the mismatching of thermal expansion coefficient between Pt and sapphire substrates. To clarify the influence of substrate temperature on Pt surface morphology, the Pt-coated sapphire substrates were annealed at different temperature for 30 min. Figure 2 presents the AFM morphologies of Pt film surface. It is interesting that the Pt electrode surface annealed at 750 °C exhibits the smoothest surface with a roughness less than 4 nm. This result shows that the Pt surface morphology deposited at lower temperature can be improved by annealing process at higher temperature. However, lots of small hills form evidently when annealed at temperature of 800 °C, indicating that the disadvantageous effect of high temperature begins to appear. Our results indicate that suitable substrate temperature for film deposition should not be higher than 750 °C. Based on the results from Figs. 1 and 2, we suggest that 750 °C of substrate temperature may be appropriate for preparing BST thin films. All BST thin films discussed below are deposited at 750 °C.

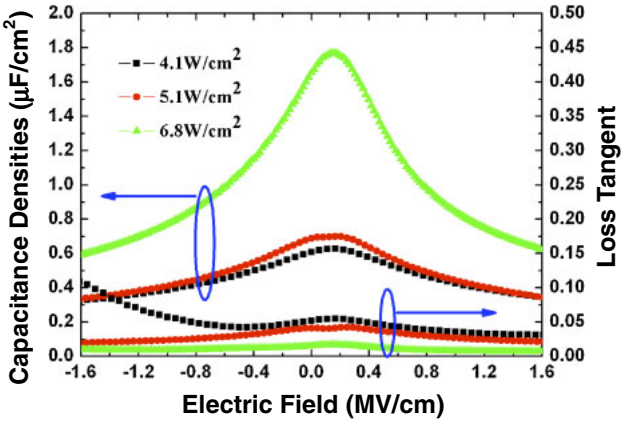

Fig. 3. (Color online) Tunability and dielectric loss of the Au/BST/Pt capacitors deposited at different sputter RF power densities.

3.2 Effect of sputtering RF power

The initial energy of sputtered particles can be simply improved by providing a larger RF power, provided that the power can be affordable for targets. Figure 3 shows the influence of sputtering RF power on tunability and dielectric loss of the Au/BST/Pt film capacitors. As a function of RF power, dielectric loss of BST thin films decreased significantly while dielectric tunability increased with the

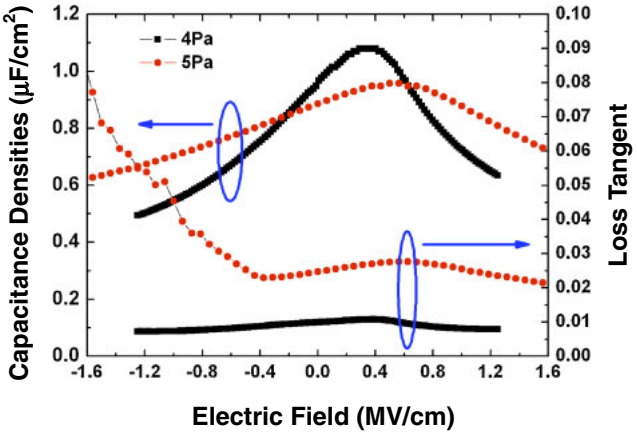

Fig. 4. (Color online) Tunability and dielectric loss of the Au/BST/Pt capacitors as a function of sputter gas pressure.

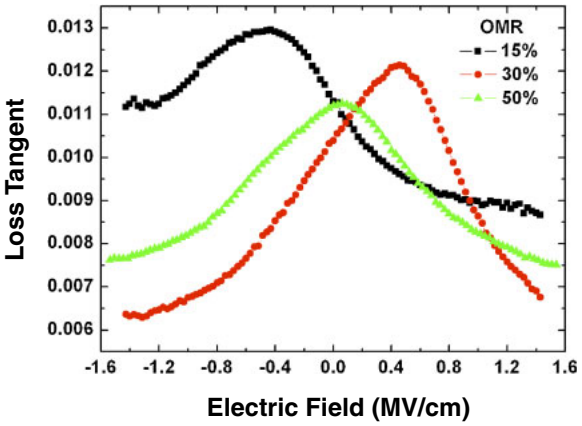

Fig. 5. (Color online) Dielectric loss of the Au/BST/Pt capacitors as a function of $O_2/(O_2 + Ar)$ mixing ratio.

increase of RF power. As expected, BST films exhibit the largest tunability and lowest loss at highest RF power density of 6.8 W/cm^2. This can be explained that high RF sputter power provides particles with a big initial energy, and finally improve the crystal quality of BST thin films.

3.3 Effect of sputtering pressure

During the particles' movement towards the substrate, their energy loss is determined by sputtering pressure. High pressure will increase the opportunity of collisions against each other, resulting in high energy loss. When particles reach substrate surface, the exchange energy decrease with increasing sputtering pressure, which is also disadvantageous for film growth. However, it does not mean that lower sputtering pressure is better. The re-sputtering will significantly enhanced and destroy film structure especially in case of high O_2/Ar mixing ratio, though high oxygen partial pressure will facilitate to decrease oxygen vacancies in BST thin films and thus reduce dielectric loss. Therefore, sputtering atmosphere deserve to be suitably selected.

The influence of sputter pressure on film dielectric properties at OMR of 50% is shown in Fig. 4. It was seen that the dielectric loss of BST thin films deposited at 4 Pa is lower than that at 5 Pa, and the tunability deposited at 4 Pa is also larger. The experimental results are greatly in accordance with our analysis presented. The particles sputtered at lower pressure have higher energy due to less energy will lose during the movement towards the substrate at a smaller probability, and high energy of particles is considered to be desirable for film crystallization and growth. However, we do not mean that lower sputter pressure is better. It is noticed that only dielectric properties of BST thin films sputtered at 4 and 5 Pa were presented. In our experiments the BST films could not even deposit on substrate at a further low pressure, i.e., 2 Pa. We believe that the etching effect on substrate surface resulting from re-sputtering at too low pressure takes an advantage over the film deposition.

Figure 5 shows the influence of OMR corresponding to oxygen partial pressure on dielectric loss of BST thin films. It is seen that the dielectric loss of thin films at zero bias is slightly decreased with the increase of oxygen partial pressure, which is believed to be a positive contribution of reduced oxygen vacancies in thin films. However, we should also expect that the excessive oxygen partial pressure would not improve the integrity of film crystallization due to the re-sputtering of oxygen negative ions. Generally, the effect of sputter atmosphere is complex, as the sputter gas pressure and OMR influence the yields of the target species, distribution, the scattering probabilities of the species by the sputter gas ions, and re-sputtering.

3.4 Result from optimized conditions

Based on above analysis and experimental results, the optimized deposition conditions with high sputter RF power, medium gas pressure and O_2/Ar ratio at appropriate substrate temperature would be favored. The Mn-doped BST thin films exhibit low dielectric loss of 0.64% and tunability of 50% at the applied electric field of 1.2 MV/cm under optimized conditions of substrate temperature at 750 °C, pressure at 4 Pa with an $O_2/(O_2 + Ar)$ mixing ratio of 50%, and sputter RF power density at 6.8 W/cm^2, as presented in Fig. 5. In this study, we suggested that by optimizing film growth conditions the film integrity of crystallization and growth as well as interfacial structure between film and bottom electrode have been improved, resulting in the reduced dielectric loss. However, the compensation for oxygen vacancy defects due to Mn^{2+} dopants might be another mechanism. To clarify the real origin of the reduced dielectric loss in Mn^{2+}-doped BST thin films observed by our results, for comparison, we deposited the un-doped thin films under the identical optimized conditions. The measured dielectric loss and tunability was also presented in Fig. 6. It is found that the un-doped BST thin films perform low dielectric loss as well, very similar to the Mn-doped ones. The results indicate that the improved dielectric properties of BST thin films in MIM configuration should be mainly attributed to the optimized film growth conditions rather than a consequence of Mn^{2+} dopants.

4. Conclusions

In conclusion, we have investigated the effects of sputtering parameters during film deposition, and the relationship between this variation in growth conditions and the electrical properties of the resulting BST thin films in parallel plate MIM capacitor structure. It was found that by carefully

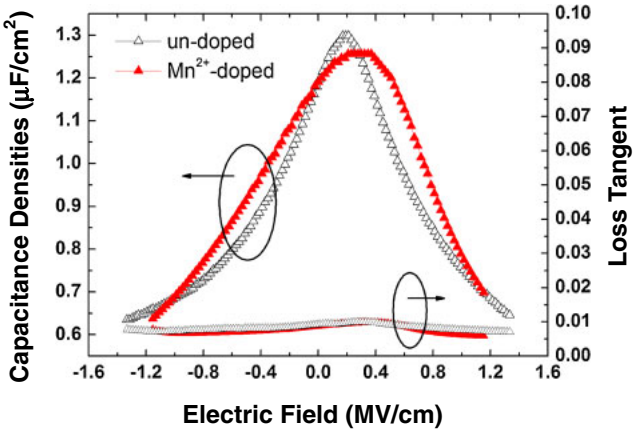

Fig. 6. (Color online) Dielectric properties comparison between doped and undoped BST thin films in Au/BST/Pt MIM configuration.

optimizing growth conditions to satisfy good integrity of film crystallization and interfacial structure we were able to deposit BST thin films with improved dielectric properties. Under optimized conditions of substrate temperature at 750 °C, pressure at 4 Pa with an $O_2/(O_2 + Ar)$ mixing ratio of 50%, and sputter RF power density at 6.8 W/cm^2, the deposited BST thin films performed a good compromise of tunability of 50% and dielectric loss of 0.64% at 1.2 MV/cm.

Of course, the mechanism behind the improvement, such as the quantity characteristic of oxygen vacancy for different deposition conditions and dopants need to be explored. Process optimization should also be further performed to improve the dielectric properties for Mn-doped BST film with a MIM configuration.

Acknowledgements

The authors would gratefully appreciate the financial support from National Natural Science Foundation of China (51172035) and the Key Program of National Natural Science of China (50932002).

1) C. L. Chen, J. Shen, S. Y. Chen, G. P. Luo, C. W. Chu, F. A. Miranda, F. W. Van Keuls, J. C. Jiang, and E. I. Meletis: Appl. Phys. Lett. **78** (2001) 652.
2) Y. Lin, J. S. Lee, H. Wang, Y. Li, S. R. Foltyn, Q. X. Jia, G. E. Collis, A. K. Burrell, and T. M. McCleskey: Appl. Phys. Lett. **85** (2004) 5007.
3) T. Yamada, P. Muralt, V. O. Sherman, C. S. Sandu, and N. Setter: Appl. Phys. Lett. **90** (2007) 142911.
4) Y. Xia, K. Yin, C. Xu, Y. Zhang, B. Xu, W. He, X. Meng, J. Yin, and Z. Liu: Appl. Phys. Lett. **92** (2008) 102906.
5) J. F. Scott: Science **315** (2007) 954.
6) H. S. Kim, T. S. Hyum, H. G. Kim, I. D. Kim, T. S. Yun, and J. C. Lee: Appl. Phys. Lett. **89** (2006) 052902.
7) H. Chen, C. Yang, B. Wang, H. Ji, and J. Zhang: J. Appl. Phys. **105** (2009) 034112.
8) S. Ito, K. Takahashi, S. Okamoto, and I. P. Koutsaroff: Jpn. J. Appl. Phys. **44** (2005) 6881.
9) K. H. Yoon, J. H. Sohn, B. D. Lee, and D. H. Knag: Appl. Phys. Lett. **81** (2002) 5012.
10) H. Chen, C. Yang, C. Fu, J. Zhang, J. Liao, and L. Hu: Appl. Surf. Sci. **254** (2008) 3175.
11) W. Chang, J. M. Pond, S. W. Kirchoefer, and J. A. Bellotti: Appl. Phys. Lett. **87** (2005) 242904.
12) B. H. Park, E. J. Peterson, Q. X. Jia, J. Lee, X. Zhang, W. Si, and X. X. Xi: Appl. Phys. Lett. **78** (2001) 533.
13) H. Chen, C. Yang, J. Zhang, B. Wang, and H. Ji: Appl. Surf. Sci. **255** (2009) 4585.
14) Z. Yuan, Y. Lin, J. Weaver, X. Chen, C. L. Chen, G. Subramanyam, J. C. Jiang, and E. I. Meletis: Appl. Phys. Lett. **87** (2005) 152901.
15) M. Jain, S. B. Majumder, R. S. Katiyar, and A. S. Bhalla: Thin Solid Films **447–448** (2004) 537.
16) M. W. Cole, E. Ngo, S. Hirsch, M. B. Okatan, and S. P. Alpa: Appl. Phys. Lett. **92** (2008) 072906.
17) M. W. Cole, E. Ngo, S. Hirsch, J. D. Demaree, S. Zhong, and S. P. Alpay: J. Appl. Phys. **102** (2007) 034104.
18) A. Podpirka, M. W. Cole, and S. Ramanathan: Appl. Phys. Lett. **92** (2008) 212906.
19) X. H. Zhu, D. N. Zheng, W. Peng, J. Li, and Y. F. Chen: Mater. Lett. **60** (2006) 1224.
20) R. Y. Kim, H. S. Kim, M. H. Lim, H. G. Kim, and I. D. Kim: Integrated Ferroelectr. **66** (2004) 195.
21) G. Subramanyam, C. L. Chen, and S. Dey: Integrated Ferroelectr. **77** (2006) 189.
22) Y. H. Fan, S. H. Yu, R. Sun, L. Li, Y. S. Yin, K. W. Wong, and R. X. Du: Appl. Surf. Sci. **256** (2010) 6531.
23) Y. Wang, B. Liu, F. Wei, Z. Yang, and J. Du: Appl. Phys. Lett. **90** (2007) 042905.
24) S. Hong, H. Bak, I. An, and O. K. Kim: Jpn. J. Appl. Phys. **39** (2000) 1796.